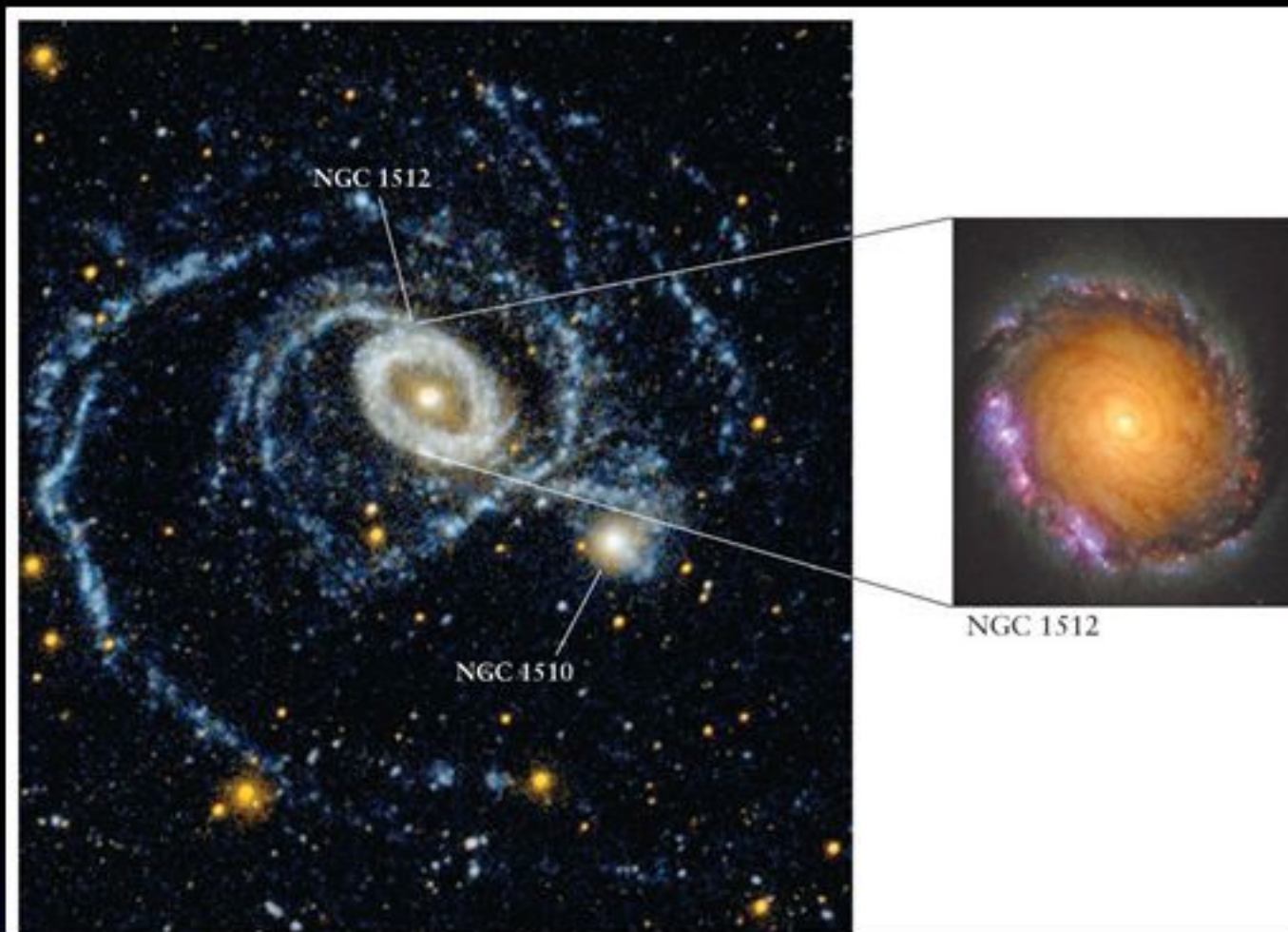




Gamma-rays from large-scale outflows in starburst galaxies

Gustavo E. Romero
(UNLP & IAR, CONICET)
HEPRO VII
July 12, 2019, Barcelona

Starburst Galaxies



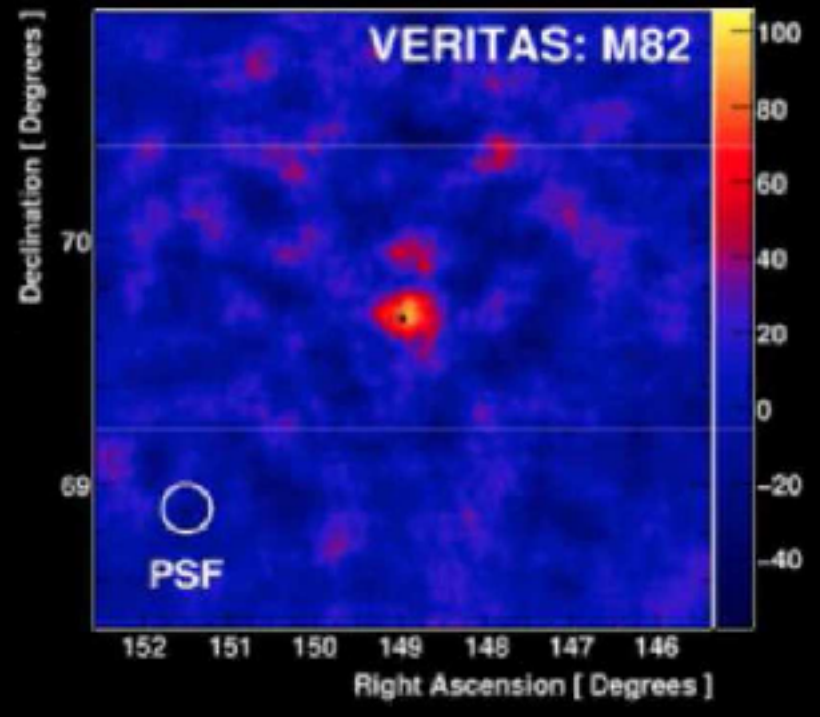
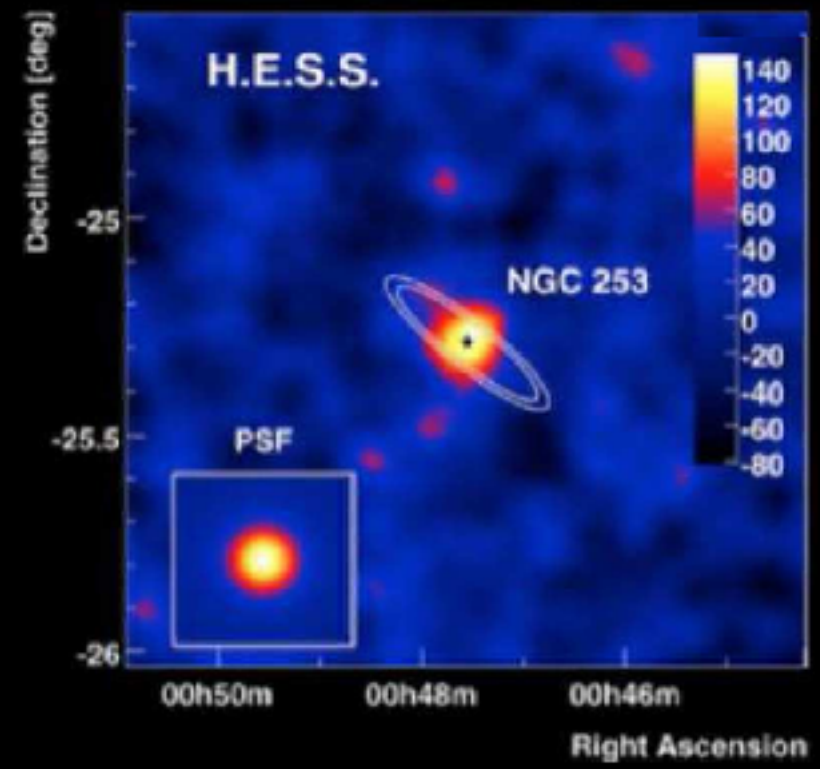
- A starburst galaxy is a galaxy undergoing an exceptionally high rate of star formation.
- Sometimes form when galaxies collide

Enhanced star formation results in:

- ❖ Large number of massive stars with strong winds.
- ❖ High infrared luminosity (from heated gas).
- ❖ High rate of supernova explosions.
- ❖ High density of cosmic rays (CRs) accelerated by the SNRs.
- ❖ Radio and gamma-ray emission produced by these CRs.

e.g. Paglione et al. 1996, Romero & Torres 2003, Torres 2004, etc...

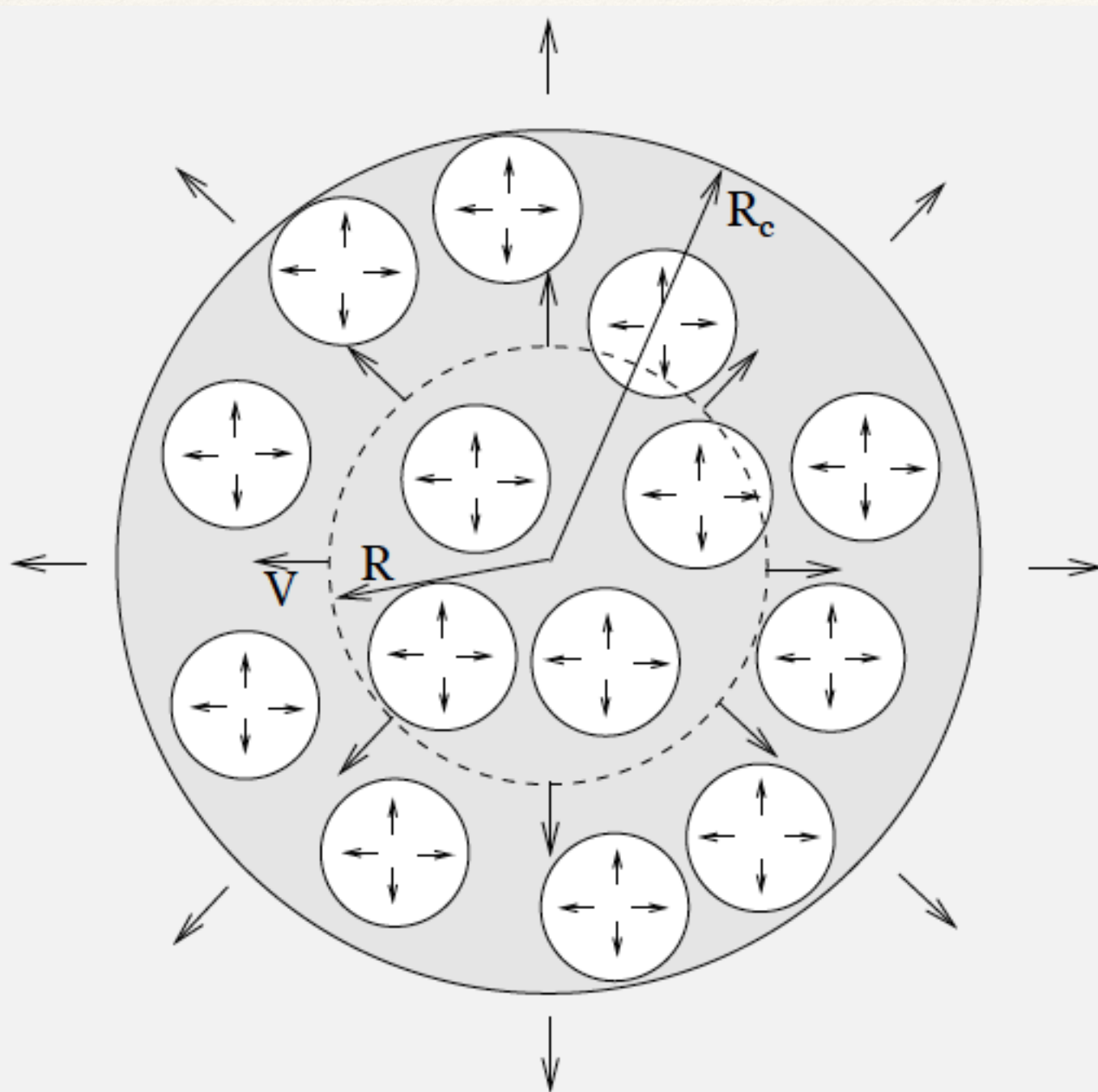
M82



NGC 253

Superwinds

The combined effect of SN and stellar winds creates a high-temperature bubble in the starburst. This hot gas escapes powering a galactic superwind.



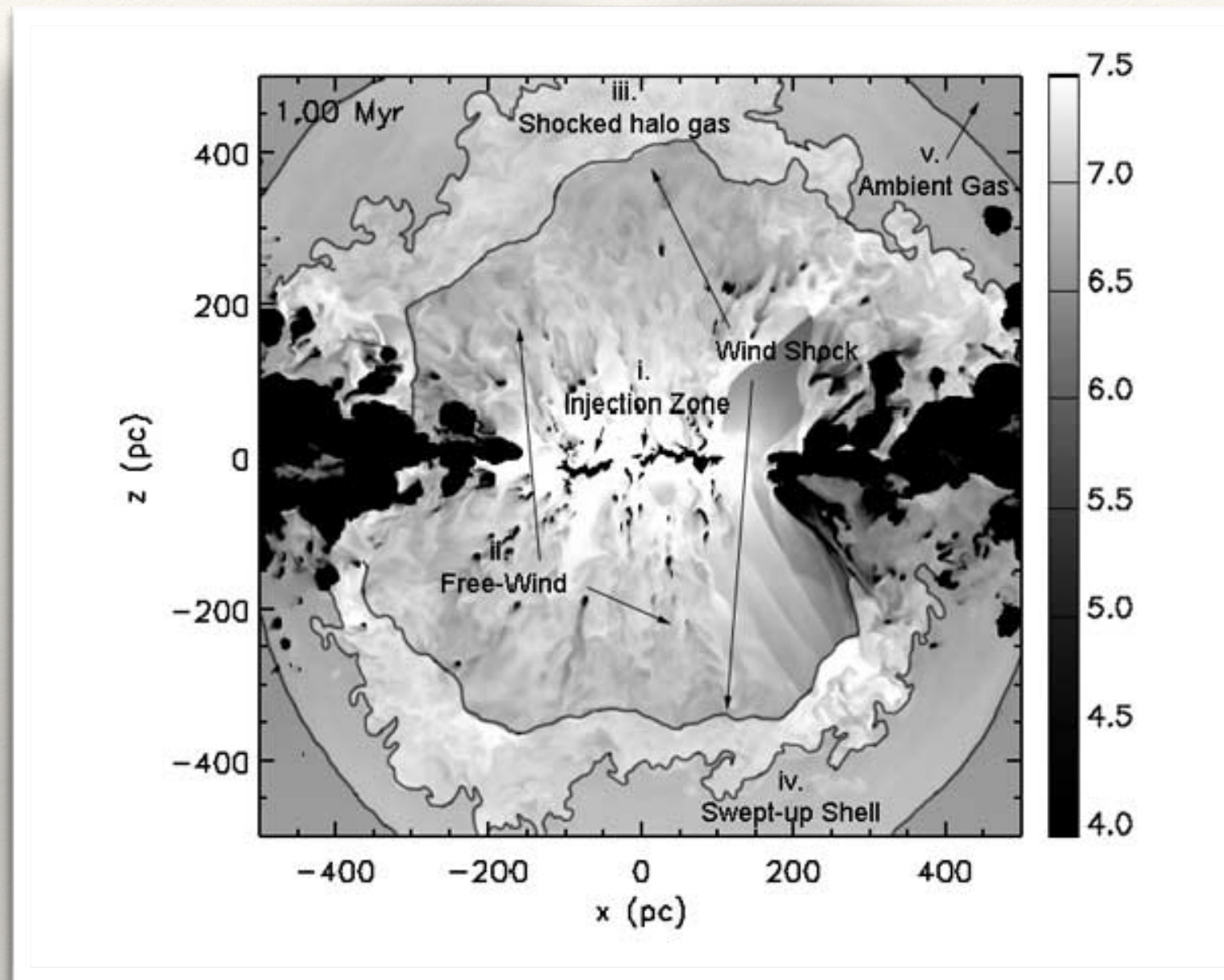
Chevallier & Clegg 1985

The large number of core-collapse supernovae in starbursts results in the merge of SNRs.

Shocks formed in these collisions thermalize the energy released by the explosions creating a cavity filled with hot ($T \sim 10^8$ K) gas that is unbound by the gravitational potential.

The hot gas expands adiabatically and escapes the system sweeping up cooler and denser gas from the disk.

Superwinds



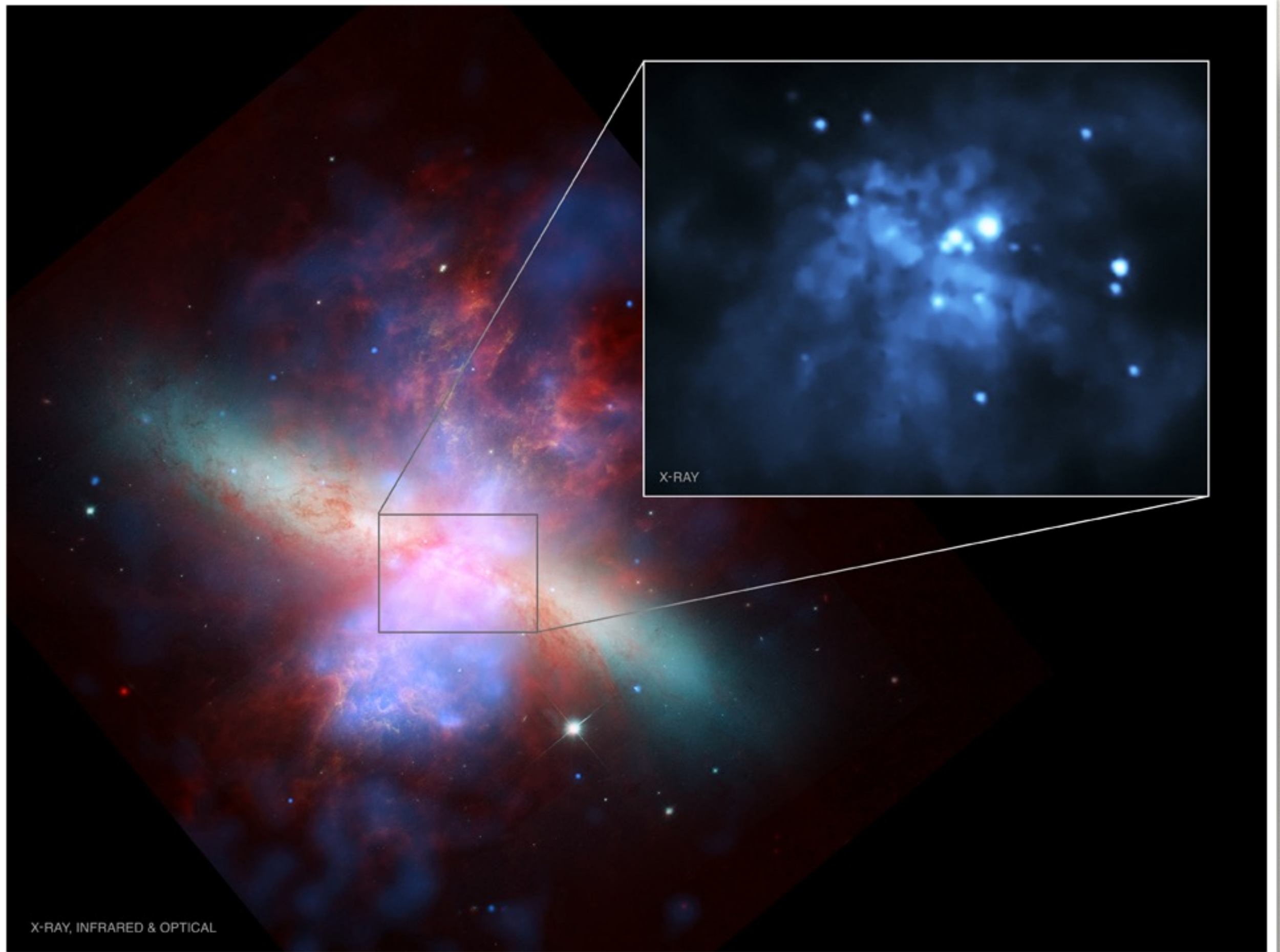
Cooper et al. 2008

Numerical simulations show that the wind expands preferentially along the minor axis of any disk-like galaxy forming a bipolar flow, sweeping up cooler, denser, ambient disk or halo gas, and stripping ambient gas from the walls of the cavity.

Superwinds

- ❖ Superwinds are complex multiphase outflows of cool, warm, and hot gas, dust, and magnetized relativistic plasma.
- ❖ Evidence for superwinds include: detection of metals in the IGM, measurements of outflows in H α and molecular lines, X-ray diffuse emission above the galaxies, radio halos, hard X-ray radiation with $T \sim 10^{7-8}$ K, etc.

M82 - Composite: *Chandra* + *HST* + *Spitzer*



Scaling relations

$$\dot{E} = \epsilon \dot{E}_*. \quad \epsilon: \text{thermalization parameter}$$

$$\dot{M} = \dot{M}_* + \dot{M}_{\text{ISM}} = \beta \dot{M}_*. \quad \beta: \text{mass load}$$

$$\dot{E}_* = 7 \times 10^{41} (\text{SFR}/M_{\odot}\text{yr}^{-1}) \text{ erg s}^{-1}$$

$$\dot{M}_* = 0.26 (\text{SFR}/M_{\odot}\text{yr}^{-1}) M_{\odot}\text{yr}^{-1}$$

$$\dot{\tau}_{\text{SN}} = 0.02 (\text{SFR}/M_{\odot}\text{yr}^{-1}) \text{ yr}^{-1}$$

$$\text{SFR} \approx 17 \frac{L_{\text{IR}}}{10^{11} \text{ erg s}^{-1}} M_{\odot} \text{ yr}^{-1}$$

As a consequence of the previous relations the outflow final velocity depends on the thermalization efficiency and the mass load factor:

$$v_{\infty} = \sqrt{\frac{2\epsilon\dot{E}_*}{\beta\dot{M}_*}} \approx 3000 \sqrt{\frac{\epsilon}{\beta}} \text{ km s}^{-1}$$

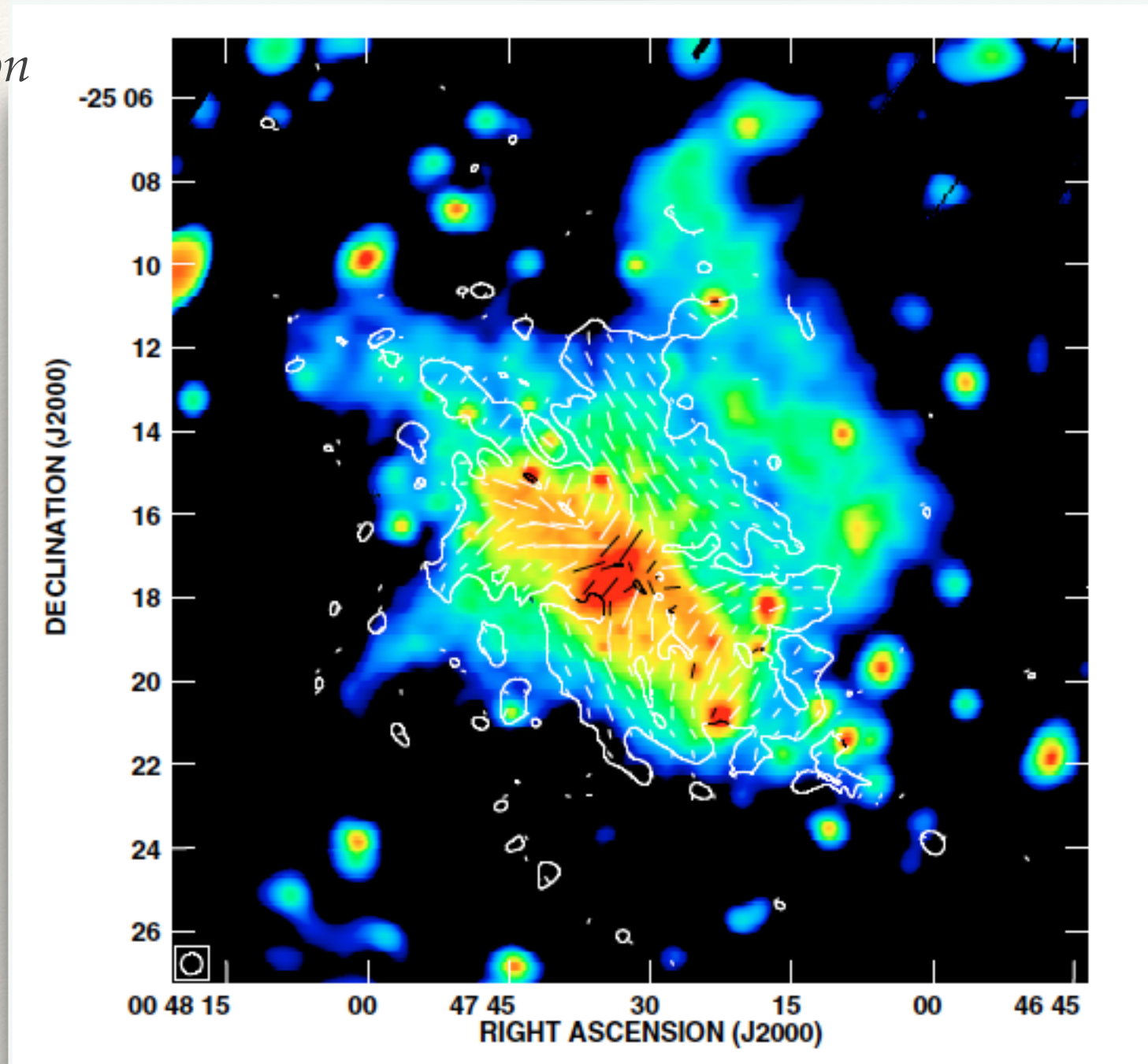
β can be determined from high-resolution CO observations.

The nearby starburst NGC 253

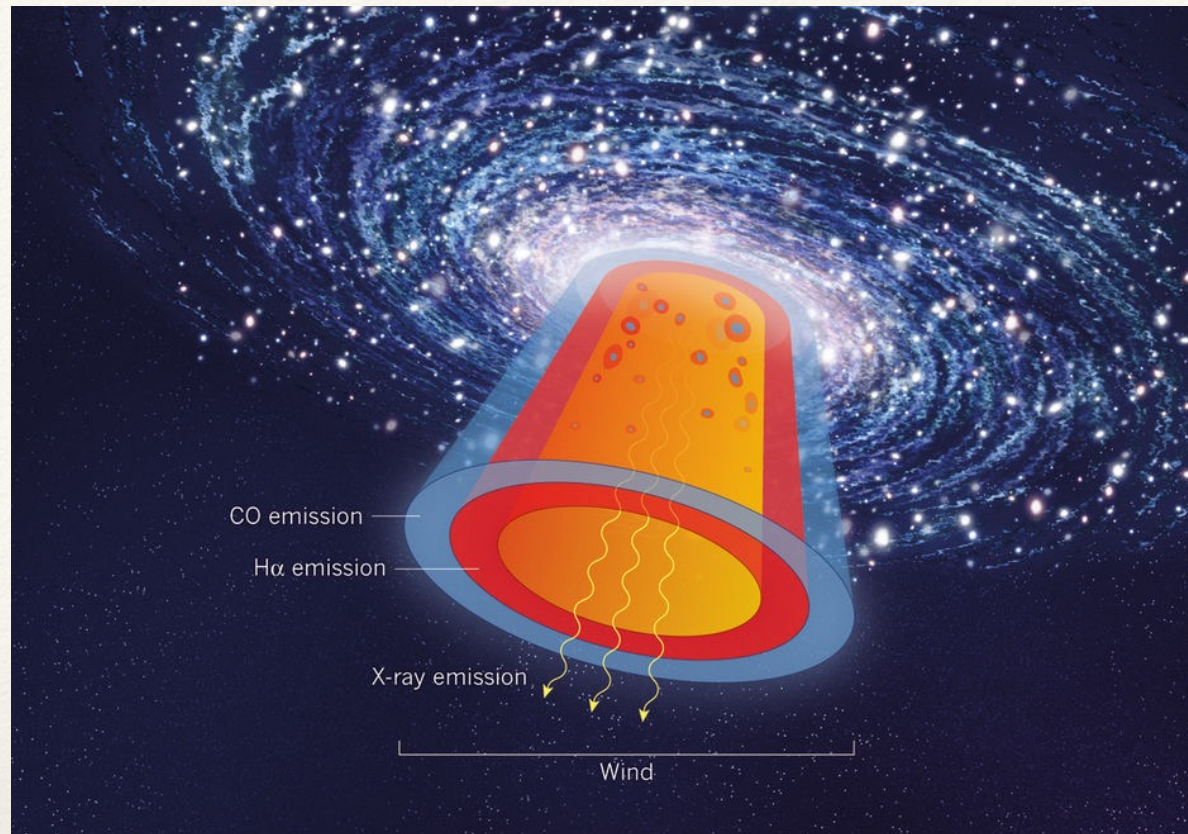
- ❖ Edge-on galaxy.
- ❖ Very nearby (~ 3 Mpc).
- ❖ High star forming rate (~ 3 solar masses / yr in the inner starburst).
- ❖ Superwind detected in X-rays, H-alpha, CO.
- ❖ Superwind is asymmetric (NW bubble stronger).
- ❖ Non-thermal radiation from the central source.
- ❖ Radio halo (also non-thermal).

Radio polarization + X-rays

VLA + XMM-Newton



Heesen et al. 2009



$$\beta \sim 12$$

Very high mass loading!!

LETTER

450 | NATURE | VOL 499 | 25 JULY 2013

doi:10.1038/nature12351

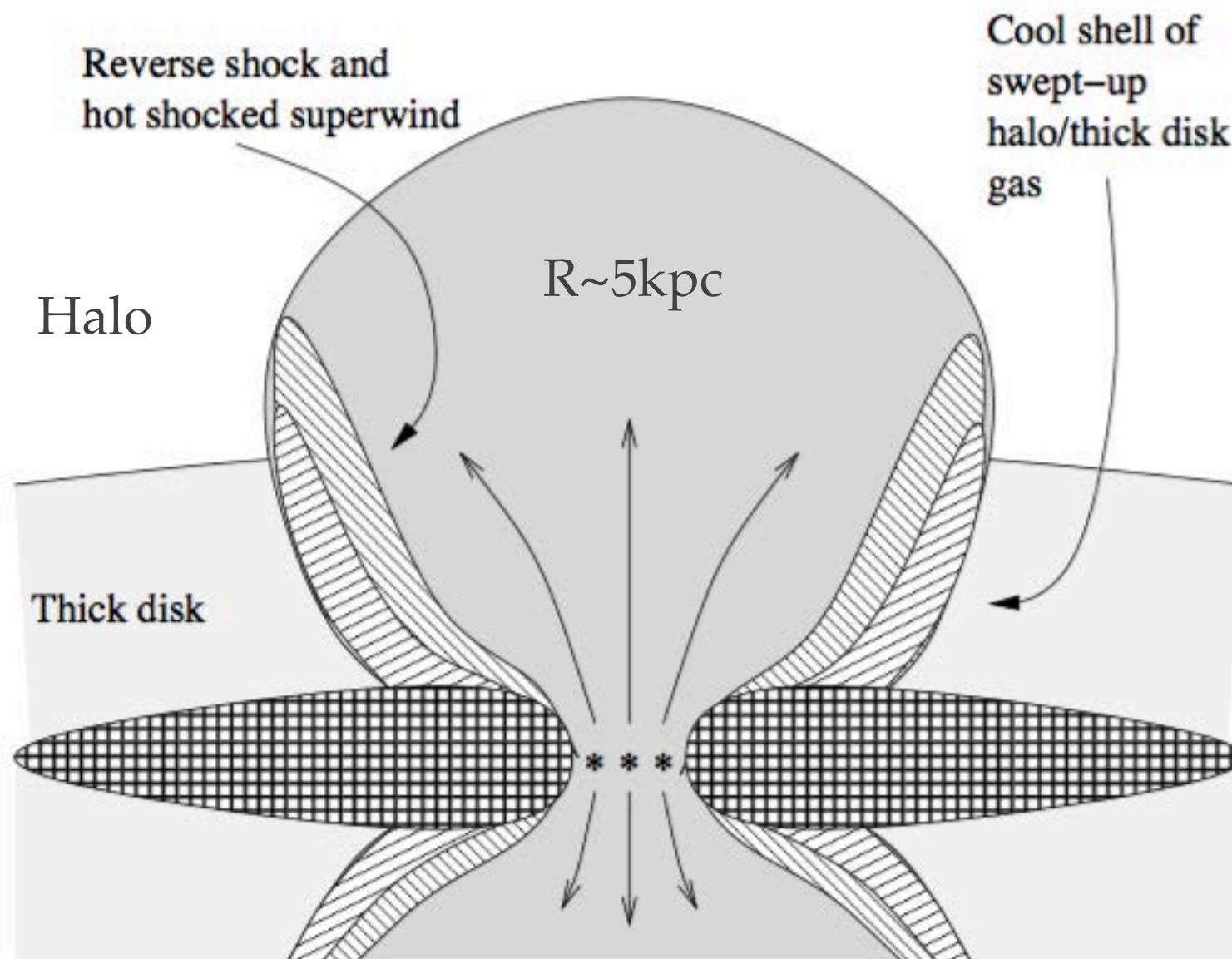
Suppression of star formation in the galaxy NGC 253 by a starburst-driven molecular wind

Alberto D. Bolatto¹, Steven R. Warren¹, Adam K. Leroy², Fabian Walter³, Sylvain Veilleux¹, Eve C. Ostriker⁴, Jürgen Ott⁵, Martin Zwaan⁶, David B. Fisher¹, Axel Weiss⁷, Erik Rosolowsky⁸† & Jacqueline Hodge³

Table 1. Physical properties of NGC 253 and its superwind.

Starburst parameters	Value
d : Distance [Mpc]	$2.6^1 - 3.9$
L_{IR} : Infrared luminosity [L_{\odot}]	1.7×10^{10}
SFR: Star forming rate [$M_{\odot} \text{ yr}^{-1}$]	3
β : Mass loading factor	12
\dot{M} : Mass outflow [$M_{\odot} \text{ yr}^{-1}$]	9
$L_{\gamma}[E > 200 \text{ MeV}]$: γ -ray luminosity [erg s^{-1}]	4.3×10^{39}
T_c : Temperature of the central region [K] ²	2×10^7
SW region parameters	Value
R : Radius of the SW bubble [kpc]	5
L_x : X-ray luminosity [erg s^{-1}]	5×10^{38}
T_h : Temperature of the gas in the bubble [K]	3×10^6
n : Particle density [cm^{-3}]	2×10^{-3}
B : Magnetic field [μG]	5
v_A : Alfvén velocity [km s^{-1}]	240
v_s : Sound speed [km s^{-1}]	164

Superwind region



- Cool halo gas
- Tenuous hot superwind (weak X-ray emitter)
- High emissivity X-ray-emitting gas ($T \sim \text{a few } 10^6 \text{ K}$)

DSA

In the NE superwind bubble:

Parameters	$\epsilon = 1$	$\epsilon = 0.75$
\dot{E} : Mechanical luminosity of the superwind [erg s ⁻¹]	1.5×10^{42}	1.1×10^{42}
v_{rev} : Velocity of the reverse shock [km s ⁻¹]	866	750
v_{shell} : Velocity of the expanding shell [km s ⁻¹]	494	407

$$\frac{dE}{dt} = \frac{3}{20} ec \left(\frac{D}{D_B} \right)^{-1} \left(\frac{v_{\text{rev}}}{c} \right)^2 B$$

$$t_{\text{acc}} \approx 2.1 \left(\frac{D}{D_B} \right) \left(\frac{v_{\text{rev}}}{1000 \text{ km s}^{-1}} \right)^{-2} \left(\frac{B}{\mu\text{G}} \right)^{-1} \left(\frac{E}{\text{GeV}} \right) \text{ yr.}$$

Losses

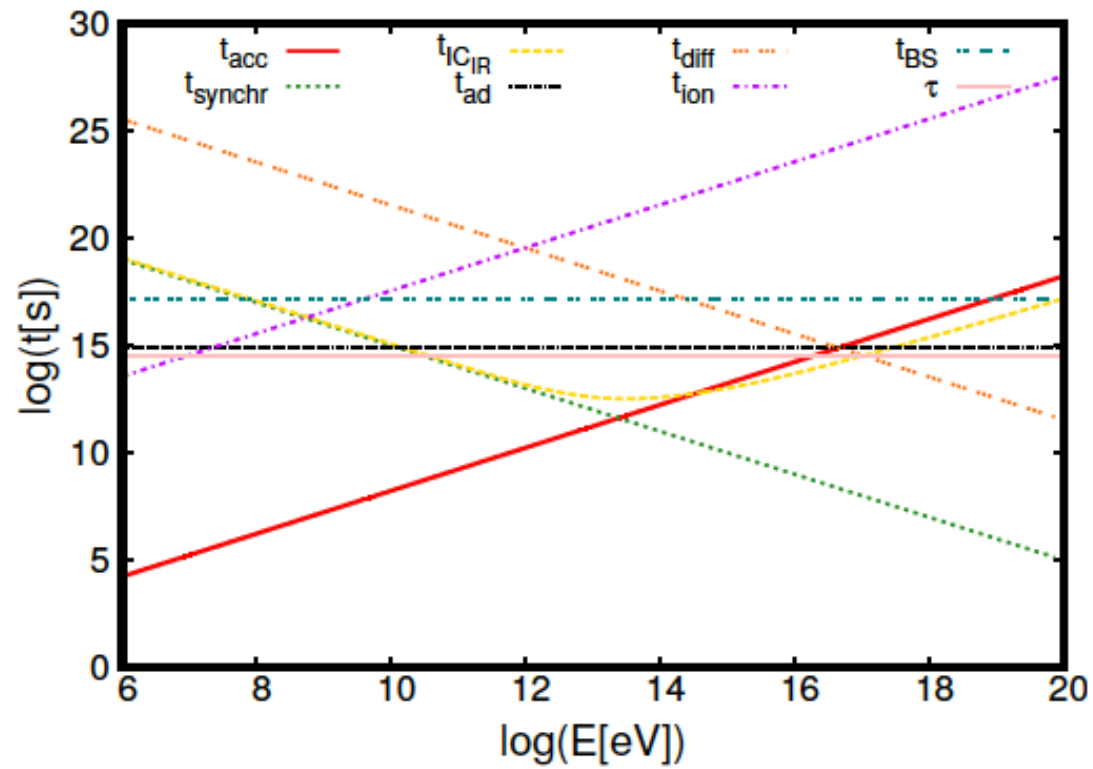


Fig. 2. Acceleration and cooling times for the electrons in a $5 \mu\text{G}$ magnetic field with a thermalization $\epsilon = 1$.

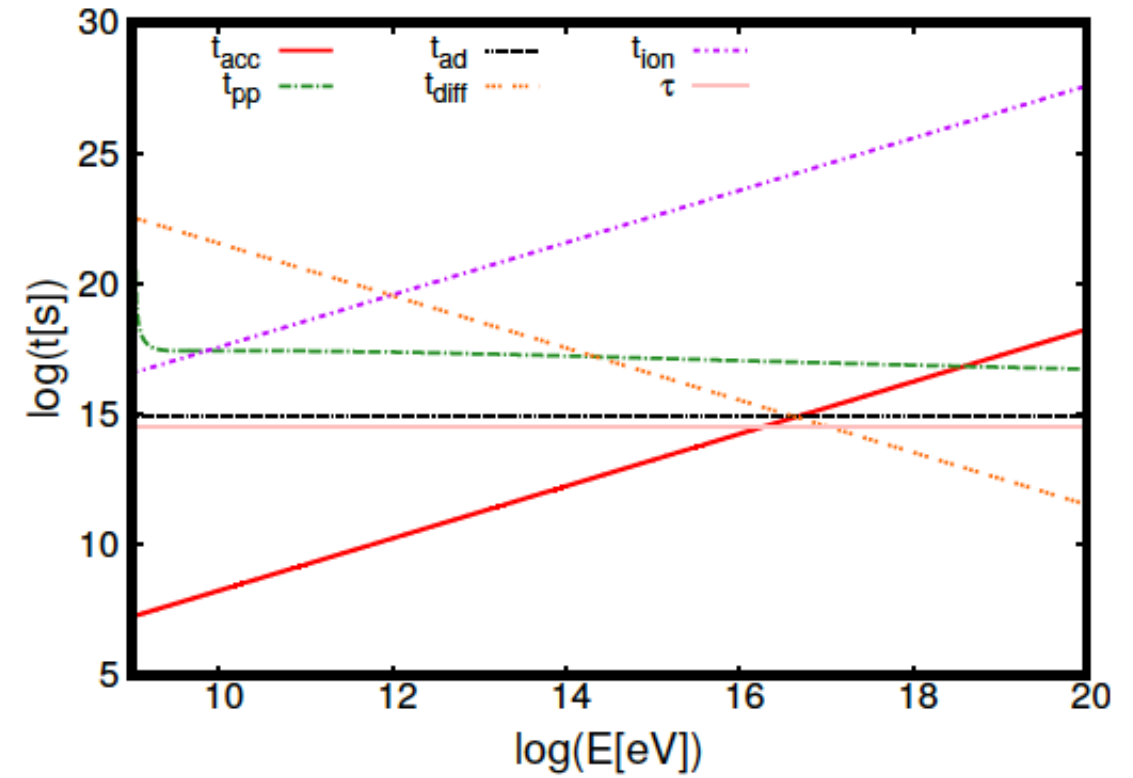


Fig. 3. Acceleration and cooling times for the protons in a $5 \mu\text{G}$ magnetic field with a thermalization $\epsilon = 1$.

For $t_{\text{acc}} = \tau$, in the Bohm limit $D = D_{\text{B}}$ and for a thermalization $\epsilon = 1$:

$$\begin{aligned} E_{\text{max}}^p &= 1.7 \times 10^{16} \text{ eV} && \text{protons} \\ E_{\text{max}}^{\text{Fe}} &= 4.4 \times 10^{17} \text{ eV} && \text{iron nuclei.} \end{aligned}$$

The CR luminosity is:

$$L_{\text{CR}} = 4\pi\xi R_{\text{shock}}^2 \rho v_{\text{shock}}^3 \sim \xi \dot{M} v_{\text{shock}}^2.$$

With an efficiency of 10%:

$$L_{\text{CR}} \sim 3.2 \times 10^{41} \text{ erg s}^{-1}$$

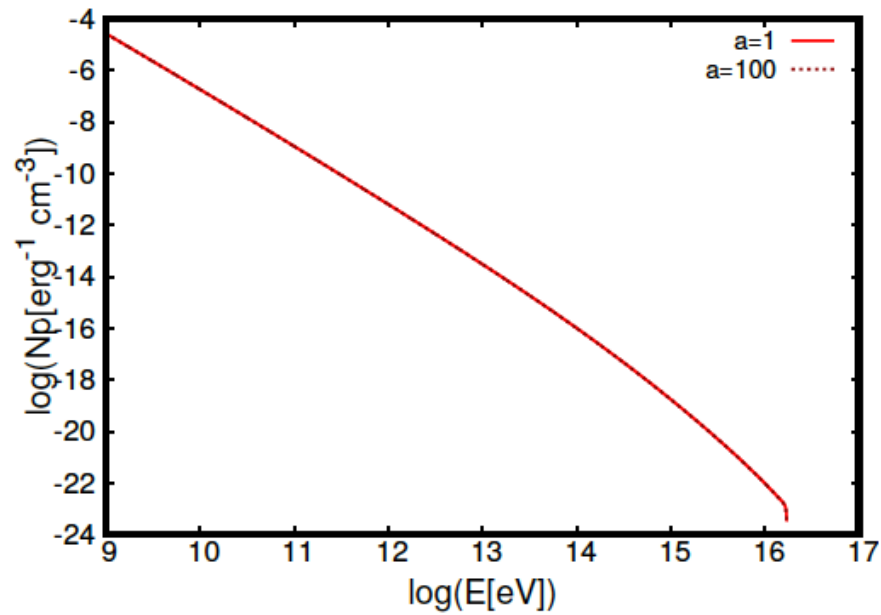


Fig. 6. Proton distributions for $a = 1$ and $a = 100$ with $a = L_p/L_e$ in the case of DSA in the reverse shock, assuming thermalization $\epsilon = 1$.

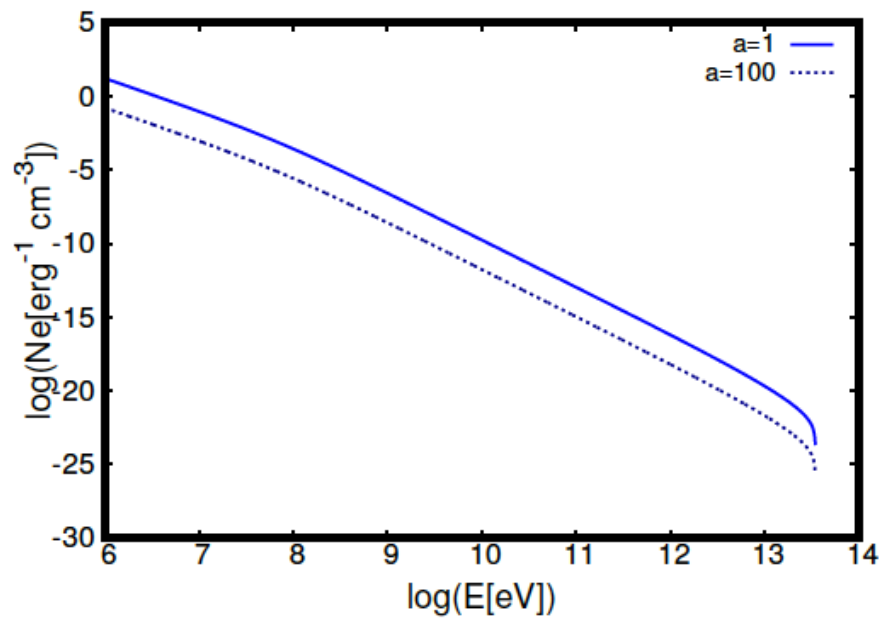


Fig. 7. Electron distributions for $a = 1$ and $a = 100$ with $a = L_p/L_e$ in the case of DSA in the reverse shock, assuming thermalization $\epsilon = 1$.

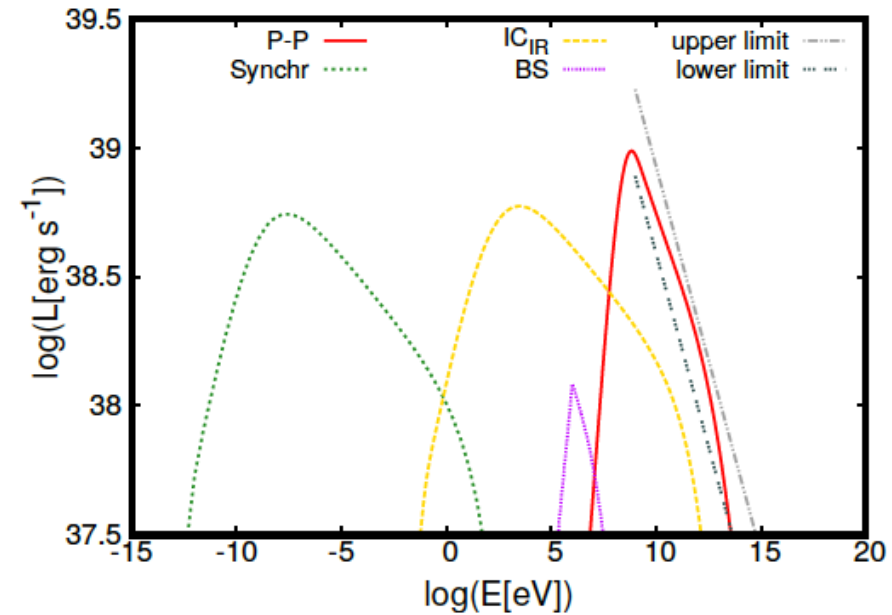


Fig. 8. Spectral energy distribution in the case of DSA with ratio $a = 1$, magnetic field $B = 5 \mu\text{G}$, thermalization $\epsilon = 1$, and shock efficiency $\xi = 0.012$.

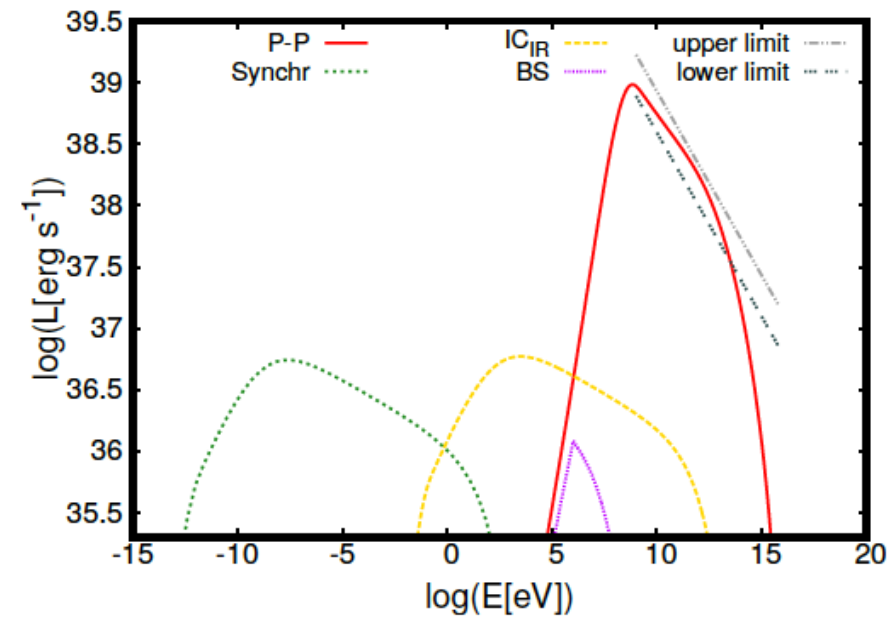
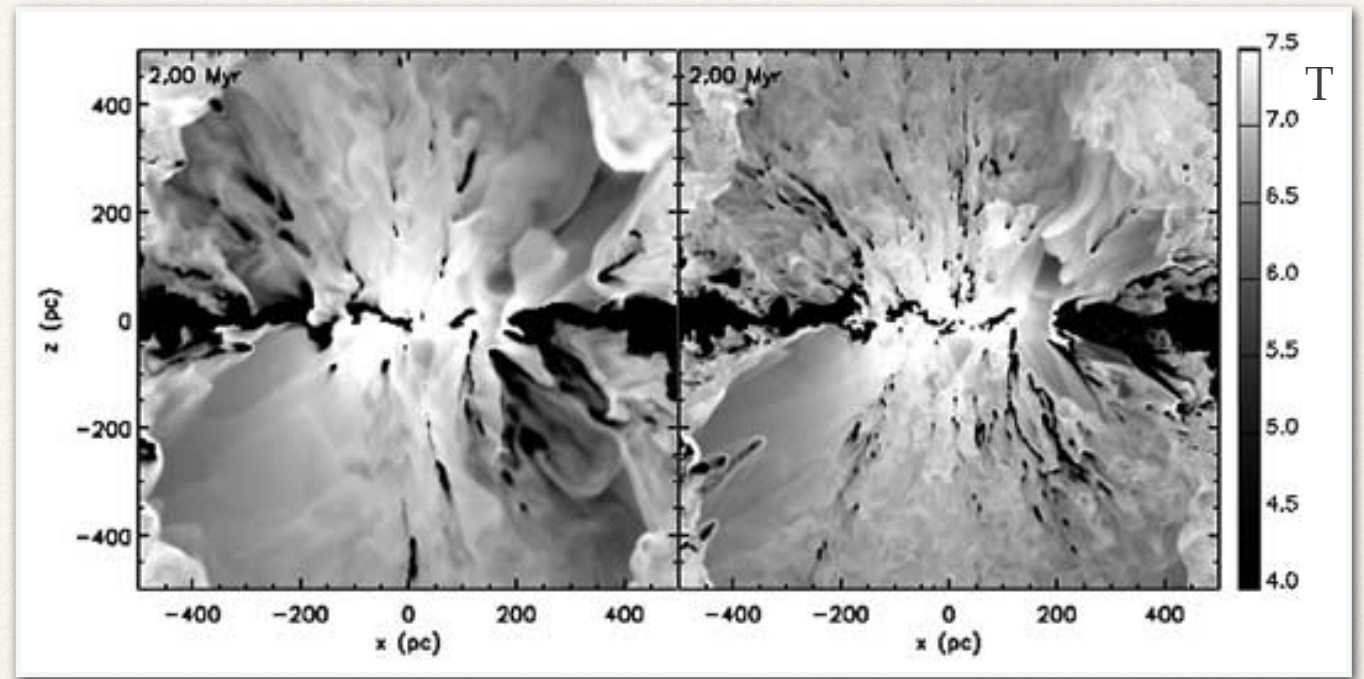
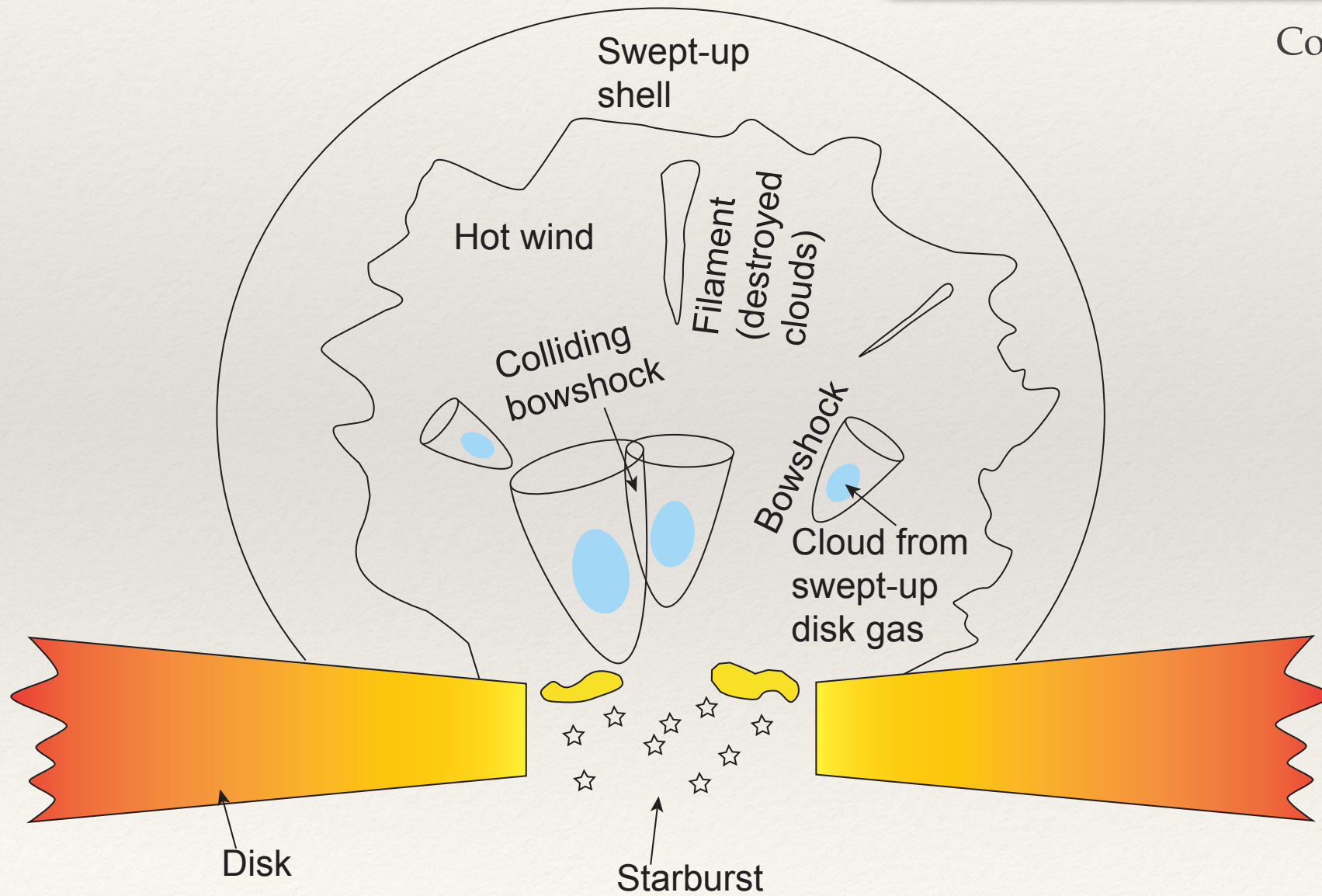


Fig. 9. Spectral energy distribution in the case of DSA with ratio $a = 100$, magnetic field $B = 5 \mu\text{G}$, thermalization $\epsilon = 1$, and shock efficiency $\xi = 6 \times 10^{-3}$.

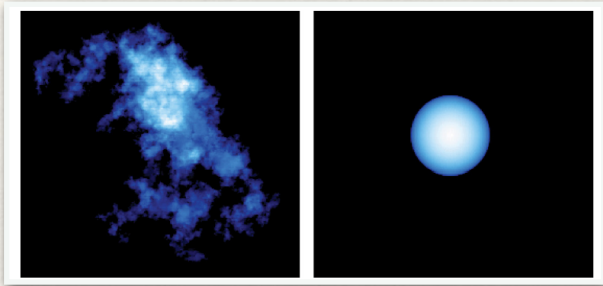
Fragments and clouds in the wind



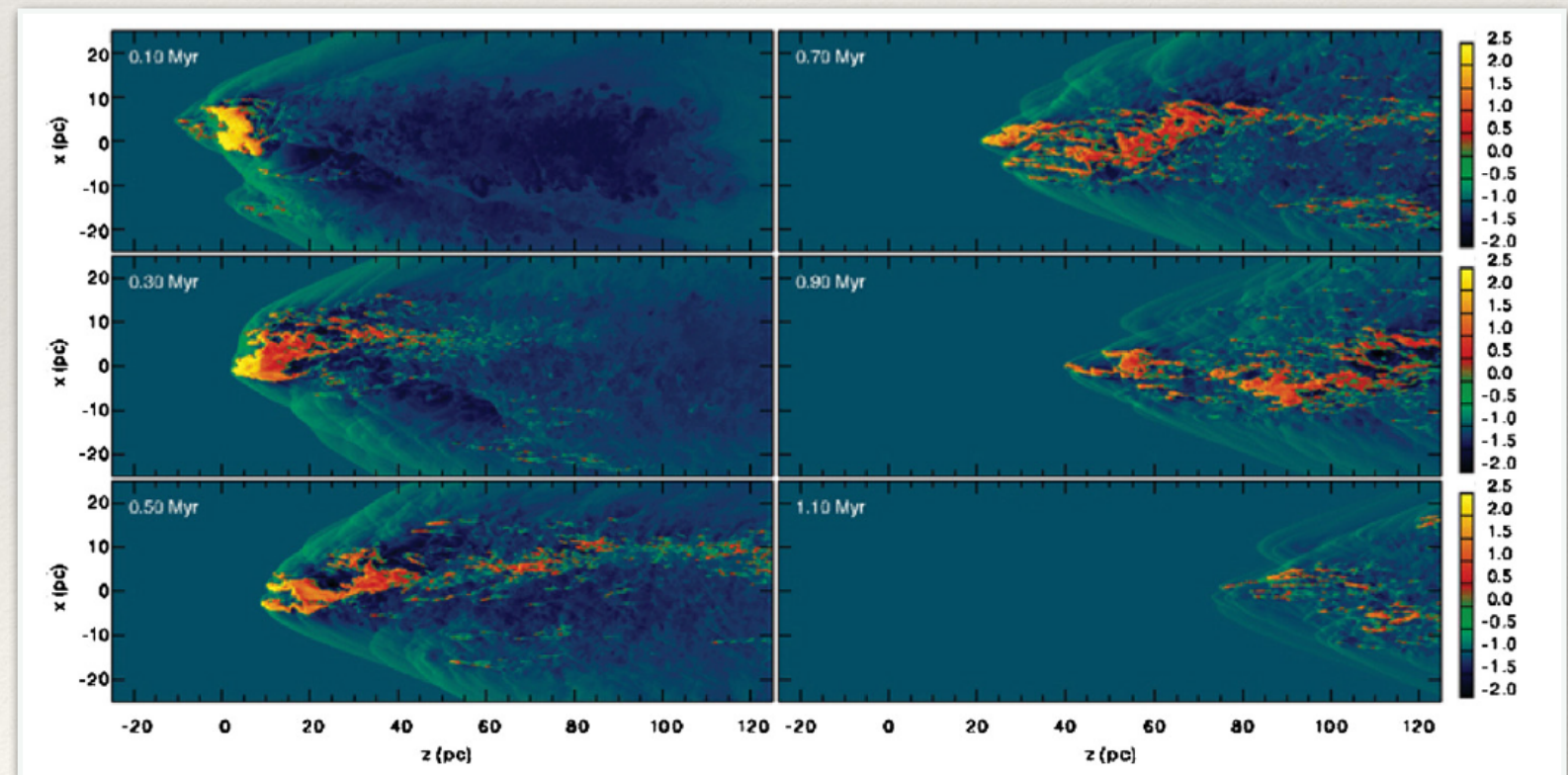
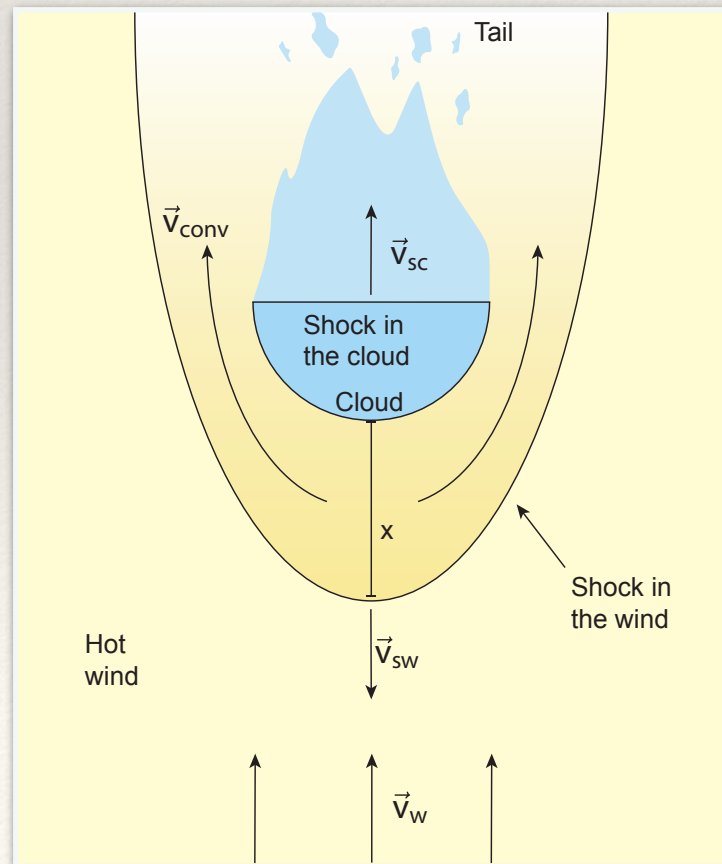
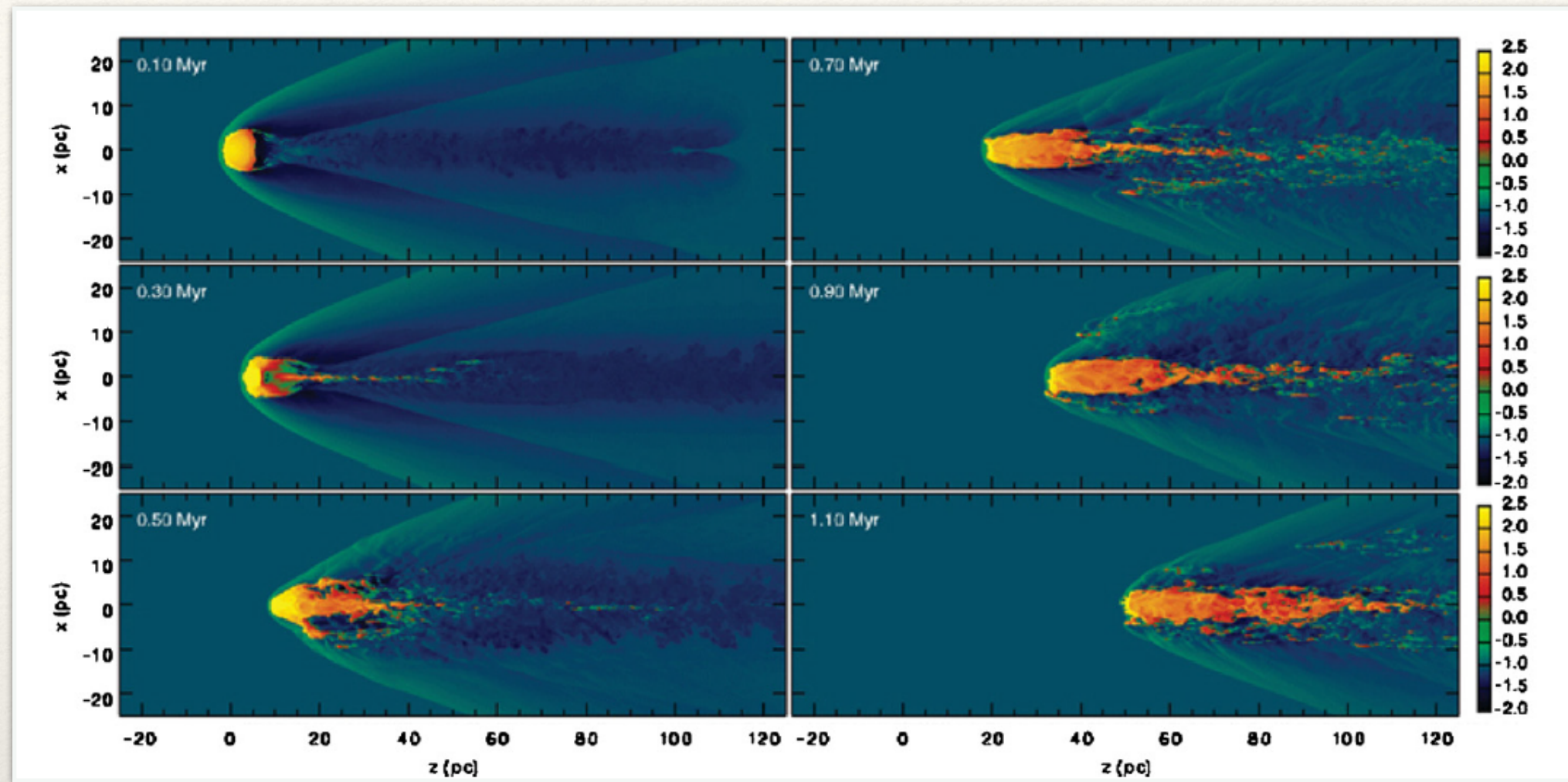
Cooper et al 2008



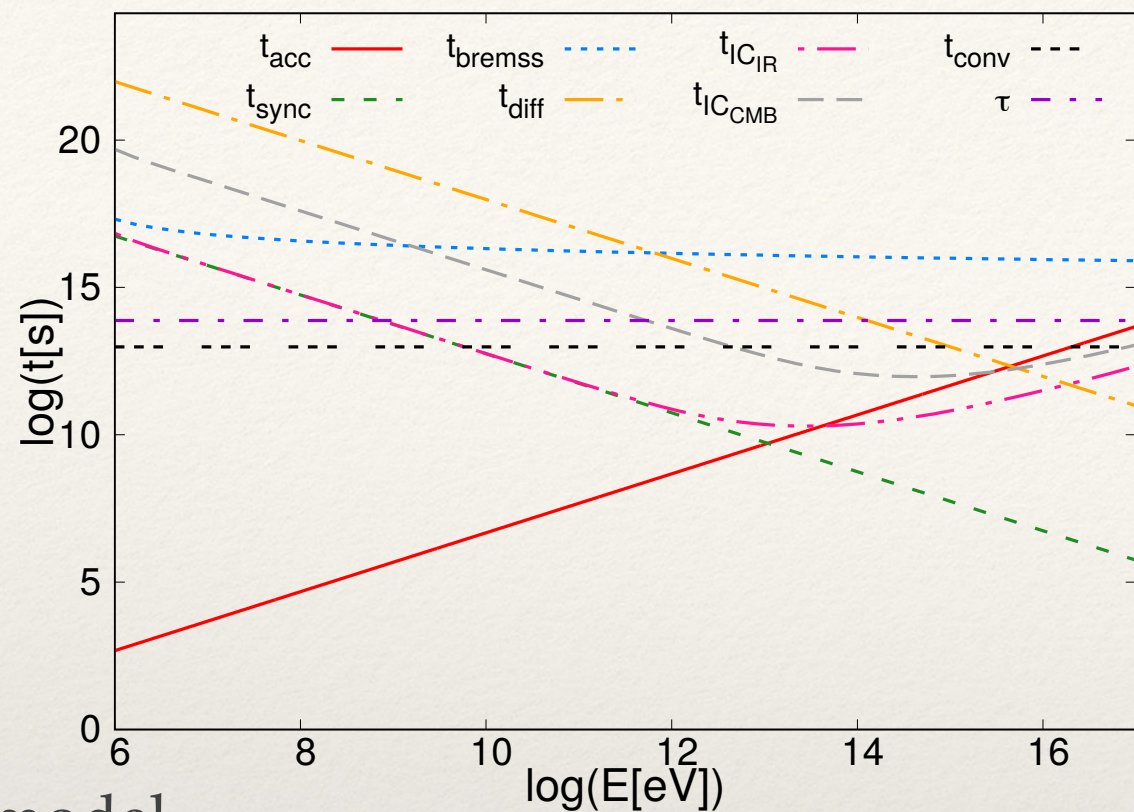
Shocked cloud



Fractal and spherical clouds: different behavior.



Losses and SEDs



M2 model

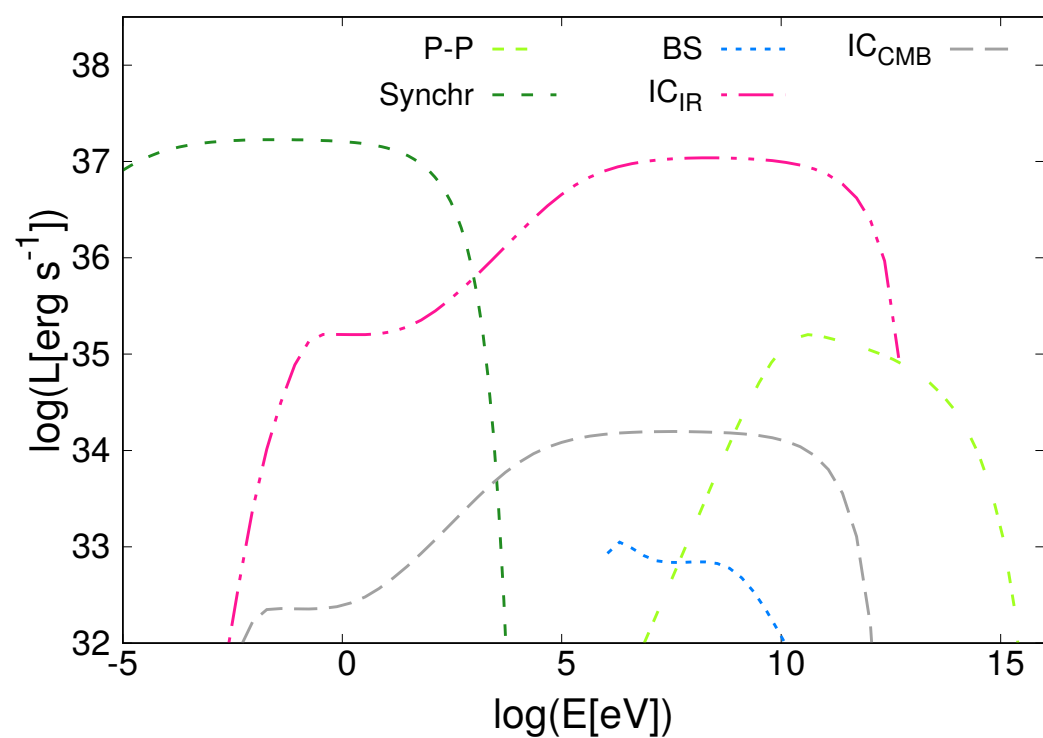
Table 1. Parameters of the models. The magnetization $\beta = 0.9$ and the wind velocity $v_w = 1000 \text{ km s}^{-1}$ are the same in both cases.

Model	R_c pc	n_w [cm^{-3}]	n_c [cm^{-2}]	v_{sw} [km s^{-1}]	v_{sc} [km s^{-1}]
M1	5	0.01	100	1320	4.2
M2	100	0.01	10	1292	13.2

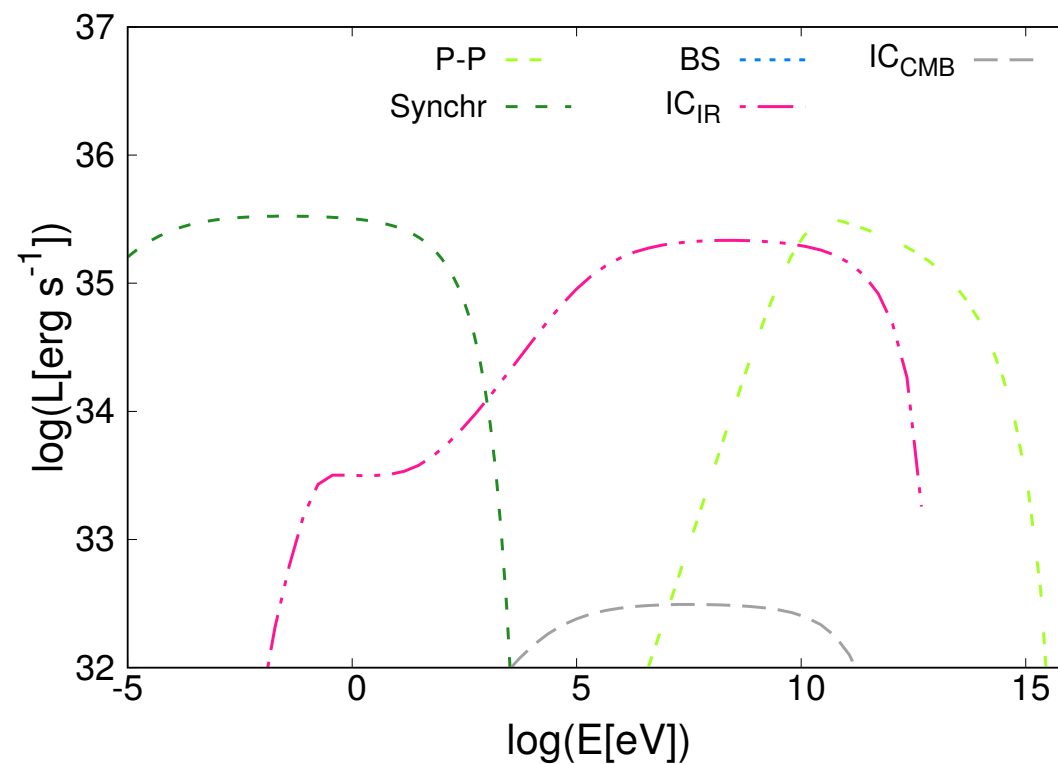
Table 2. Dynamical timescales

Model	t_{crush} [Myr]	t_{KH} [Myr]	t_{RT} [Myr]	$t_{\Lambda_{sc}}$ [Myr]	$t_{\Lambda_{sw}}$ [Myr]
M1	0.37	0.49	0.37	1.15×10^{-3}	64.78
M2	2.39	3.09	2.39	1.46×10^{-5}	60.53

a=1



a=100



Conclusions

- ❖ NGC 253 and other starbursts are sources of CRs below the Ankle in the CR spectrum.
- ❖ Gamma rays up to 10^{15} eV can be produced in the halo. This emission can be as important as emission from the disk, but reaching higher energies.
- ❖ Discrete gamma-ray sources should exist in the halo because of the interaction of the superwind with fragments of the disks.
- ❖ Some X-ray sources in the halo might be also associated with such a phenomenon as well.

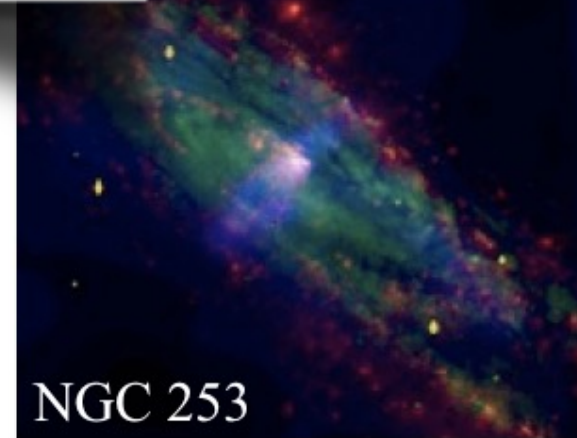
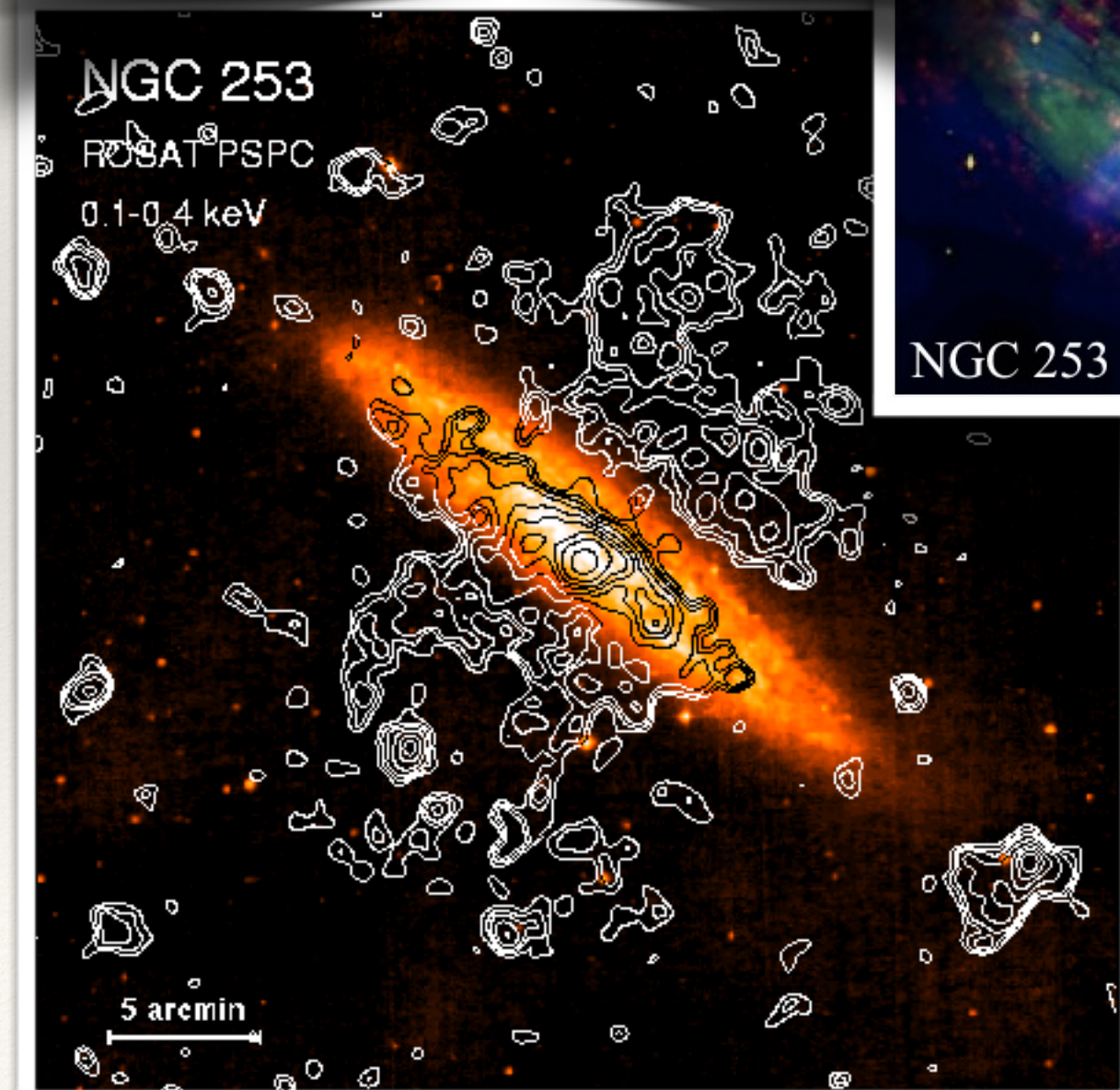
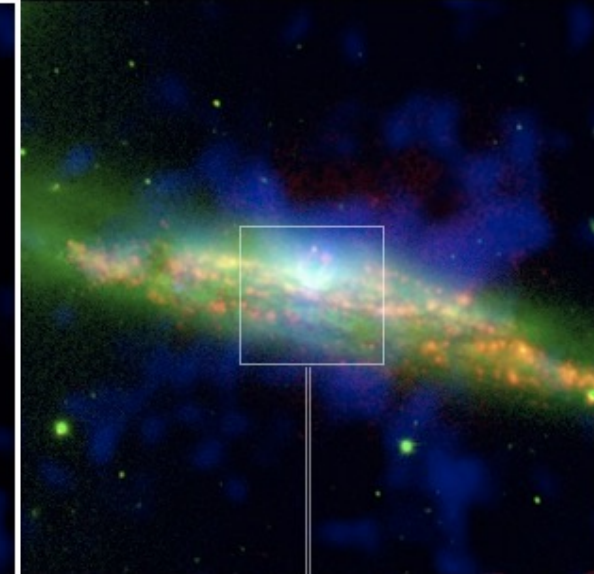
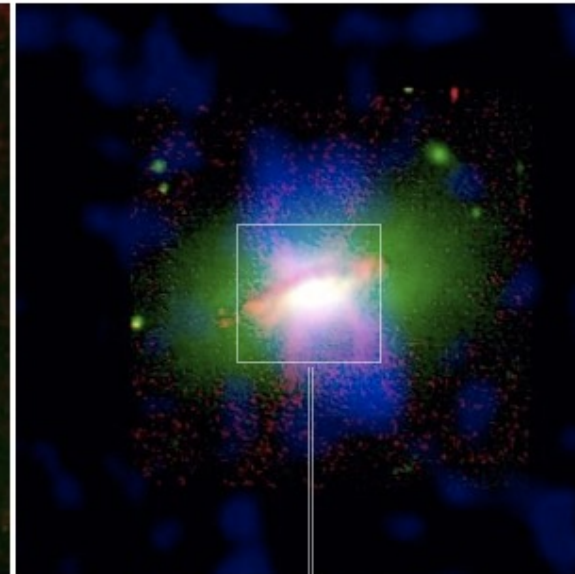
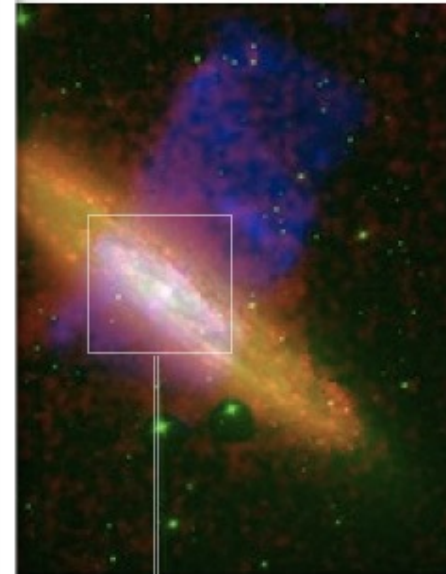


Thanks!

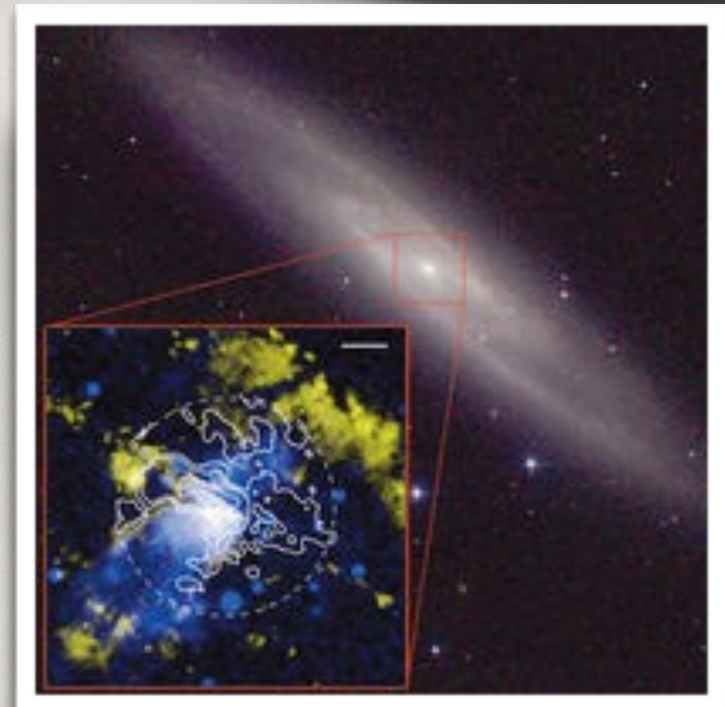
Galaxy winds driven by star formation

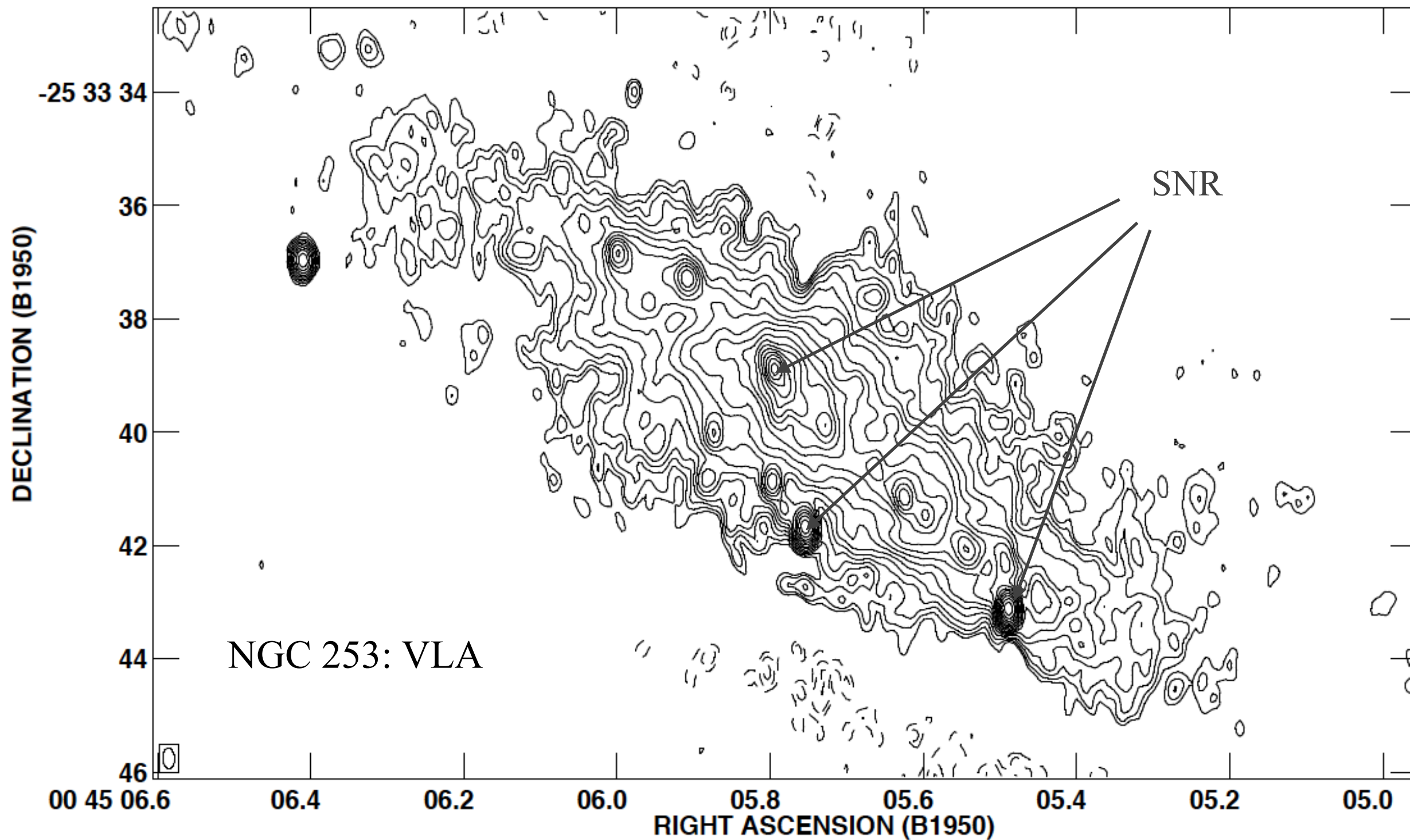


Halpha - M82



CO - NGC 253

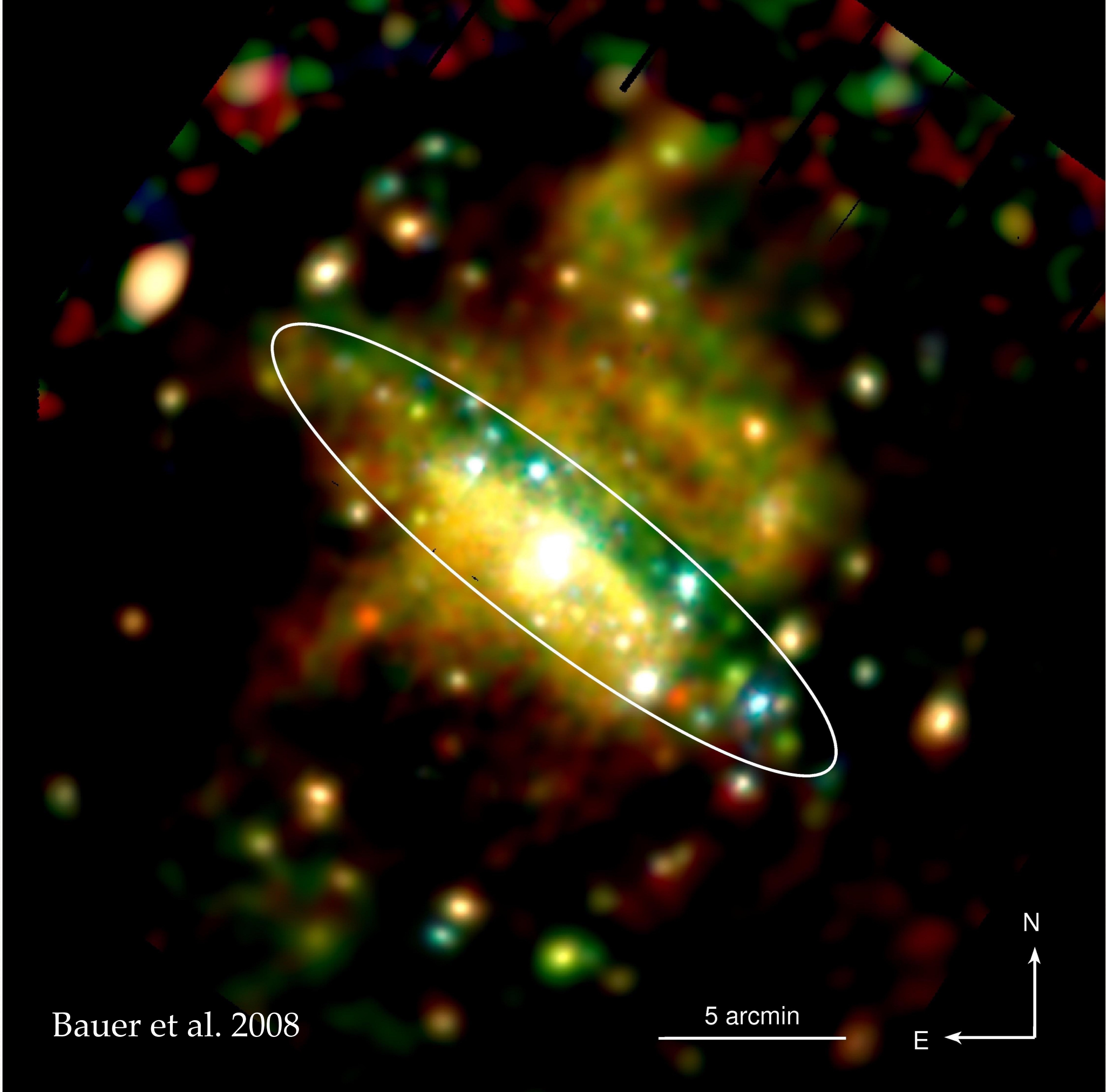




Cont peak flux = 5.5613E-02 JY/BEAM
 Levs = 9.0000E-05 * (-2.00, -1.40, -1.00,
 1.000, 1.400, 2.000, 2.800, 4.000, 5.700,
 8.000, 11.30, 16.00, 22.50, 32.00, 45.00,
 64.00, 90.00, 128.0, 181.0, 256.0, 363.0,
 512.0)

FIG. 7.—A configuration image at 3.6 cm. Contours are at logarithmic intervals of $2^{1/2}$, beginning at $0.09 \text{ mJy beam}^{-1}$.

XMM-Newton
X-rays



Bauer et al. 2008

5 arcmin

